International Journal of Computer Assisted Radiology and Surgery (2018) 13:1937–1948
https://doi.org/10.1007/s11548-018-1838-z

ORIGINAL ARTICLE

Accuracy assessment of wireless transponder tracking in the operating room environment

Roeland Eppenga[1] · Koert Kuhlmann[1] · Theo Ruers[1,2] · Jasper Nijkamp[1,3]

Received: 29 January 2018 / Accepted: 27 July 2018 / Published online: 11 August 2018

Abstract

Purpose To evaluate the applicability of the Calypso® wireless transponder tracking system (Varian Medical Systems Inc., USA) for real-time tumor motion tracking during surgical procedures on tumors in non-rigid target areas. An accuracy assessment was performed for an extended electromagnetic field of view (FoV) of 27.5 × 27.5 × 22.5 cm (which included the standard FoV of 14 × 14 × 19 cm) in which 5DOF wireless Beacon® transponders can be tracked.

Methods Using a custom-made measurement setup, we assessed single transponder relative accuracy, absolute accuracy and jitter throughout the extended FoV at 1440 locations interspaced with 2.5 cm in each orthogonal direction. The NDI Polaris Spectra optical tracking system (OTS) was used as a reference. Measurements were taken in a room without surrounding distorting factors and repeated in an operating room (OR). In the OR, the influence of a carbon fiber and regular stainless steel OR tabletop was investigated.

Results The calibration of the OTS and transponder system resulted in an average root-mean-square error (RMSE) vector of 0.03 cm. For both the standard and extended FoV, all accuracy measures were dependent on transponder to tracking array (TA) distances and the absolute accuracy was also dependent on TA to OR tabletop distances. This latter influence was reproducible, and after calibrating this, the residual error was below 0.1 cm RMSE within the entire standard FoV. Within the extended FoV, this residual RMSE did not exceed 0.1 cm for transponder to TA distances up to 25 cm.

Conclusion This study shows that transponder tracking is promising for accurate tumor tracking in the operating room. This applies when using the standard FoV, but also when using the extended FoV up to 25 cm above the TA, substantially increasing flexibility.

Keywords Accuracy assessment · Electromagnetic tracking · Surgical navigation · Wireless tracking · Surgical oncology · Abdominal surgery

Introduction

For surgical planning and guidance of surgical interventions, surgical navigation can be used. It has become part of the daily routine in a variety of fields, e.g., neurological, orthopedic, ear and facial surgical procedures [1–4]. In these fields, most navigation techniques assume there are no anatomical changes between preoperative imaging and the actual situation during the surgical procedure. This assumption does not apply to procedures in non-rigid areas such as the breasts and the abdomen, in which the anatomy changes constantly due to several factors such as breathing, organ deformation and surgical manipulation [5]. Therefore, there is a demand for soft tissue registration techniques.

Point-based registration has been studied as a possible soft tissue registration technique for image-guided liver surgery, where preoperative computed tomography (CT) images were projected onto intraoperative ultrasound (US) images [6, 7]. With this technique, anatomical landmarks are identified during the surgical procedure and subsequently registered to the corresponding points visible on preoperative imaging. However, any motion or deformation after registration requires re-registration, hampering intraoperative usability.

✉ Jasper Nijkamp
j.nijkamp@nki.nl

1 Department of Surgical Oncology, The Netherlands Cancer Institute, Amsterdam, The Netherlands

2 Nanobiophysics Group, MIRA Institute, University of Twente, Enschede, The Netherlands

3 Department of Surgery, The Netherlands Cancer Institute, Plesmanlaan 121, 1066 CX Amsterdam, The Netherlands

Alternatively, soft tissue registration can be performed of autosegmented anatomical features on intraoperative US with those corresponding on preoperative imaging [8]. Preoperative imaging can then be projected real-time onto US imaging by tracking the US probe. This technique reduces the effect of anatomical motion, but deformation of the anatomical features directly influences the registration accuracy. Surface registration techniques, in which systems such as stereo cameras continuously acquire intraoperative data over a large surface and match it with preoperative 3D models [9–11], can allow for continuous registration. For these techniques algorithms are being developed to compensate for anatomical deformations [12, 13], even when sparse intraoperative data are available [14]. However, some form of intraoperative manual registration is still required.

A more direct approach is to use easy-to-track surrogates for locating the target. Examples of these surrogates are optical markers, placed intraoperatively close to the target, and electromagnetically (EM) tracked needles or wired EM sensors implanted in or around the target [15, 16]. Once attached or implanted, intraoperative imaging techniques, such as cone beam CT (CBCT) or US, are used to find the relative position and orientation of the target with respect to the markers or sensor(s). The target motion can be tracked just by tracking these markers or EM sensors. Tracking with EM sensors has the advantage over tracking optical markers because it does not require a line of sight between sensor and tracker [17, 18]. Up to now, EM trackers used for this purpose are wired. This makes them prone to breaking, may induce sensor migration and makes preoperative implantation difficult, because of possible inconvenience for the patient.

A solution may be found in an EM tracking technique using wireless passive transponders which can be implanted preoperatively [16]. Currently, the only clinically approved system using this transponder tracking technique is the Calypso's *GPS for the Body*® technology (Varian Medical Systems Inc., Palo Alto, California, USA). This system has been widely studied on targeting accuracy and usability in radiotherapy (RT) [19–23]. Although the transponder system is designed and approved only for RT application, studies have shown its potential for surgical applications [24–26]. The main advantage using implanted transponders for surgery is in the workflow, which can be copied from RT. Based on diagnostic imaging a patient is planned for surgery and the target can be segmented. The transponders can be implanted at the radiology department under US guidance. In the days before surgery a CT scan is acquired to assess the transponder locations with respect to the tumor segmentation. In the OR, only the transponder locations need to be measured in order to estimate where the target borders are. Recently, transponder-based surgery on breast phantoms was evaluated in a pilot study and compared with iodine seed-guided surgery [26]. Results were promising, especially in more complicated tumor shapes, and surgeons were enthusiastic about the possibilities. The breast phantom study was conducted in a research environment with minimal distortion of the EM-based tracking. To further investigate the potential of a navigation setup using transponders for tumor tracking in surgical procedures, this setup has to be translated to the more challenging OR environment. In this study we focused on application in surgical procedures in the pelvic area.

With the Calypso system, transponders are detected by a sensor array integrated into the EM field generator exciting the transponders. In an RT setting, this tracking array (TA) is positioned above the patient such that an optical tracking system, mounted to the ceiling, can detect it and align the linear accelerator. However, in the OR the TA cannot be positioned above the patient as it would block the surgeon. When positioned below the patient, the TA will be close to the OR tabletop, and because EM tracking is known to be distorted in proximity of most OR tabletops, this can significantly lower the accuracy [27]. When this distortion is reproducible, calibration can solve this effect.

With the TA underneath the patient, care should be taken when positioning the patient, because the implanted transponders should be within the tracking volume of the TA and stay there for the rest of the navigated procedure. This can be rather challenging with the limited field of view (FoV) of the clinical transponder system which is $14 \times 14 \times 19$ cm. The tracking volume of the research transponder system is substantially larger, about $27.5 \times 27.5 \times 22.5$ cm. It is, however, unknown how accurate the transponders can be tracked within this extended volume. For assessing the relative accuracy a standardized protocol is available [28]. For the surgical application, an additional tracking system is used to track surgical tools besides the tumor [26]. The transponder system cannot be used to track surgical tools, because all three available transponders are used to assess the position and orientation of the tumor. When combining two tracking systems into one navigation application, absolute accuracy needs to be known as well. This measure indicates how accurately the transponder system can be calibrated with another tracking system, to correctly display where the surgical tool is with respect to the tumor. We used the NDI Polaris Spectra optical tracking system (Northern Digital Inc, Waterloo, Canada) as a reference for the absolute accuracy and could therefore also be evaluated as a possible system for tracking surgical tools.

In this study we assessed the absolute and relative tracking accuracy of the transponder system in the OR, where the TA is positioned below the patient and transponders are tracked within the clinical and extended FoV. Two types of OR tables were investigated, and measurements were repeated to assess the reproducibility of distortion for further calibration. As a reference for all OR measurements, accuracy was also assessed in a distortion free room (DFR).

Materials and methods

Hardware

The transponder system

The transponder tracking system consists of a console, a real-time readout system, an EM Field Generator/Tracking Array (TA) and three 5DOF implantable wireless Beacon® transponders of size 8 mm × 1.85 mm [29]. The clinically approved transponder system used in radiation oncology requires that the transponders have to be within a tracking volume of 14 × 14 × 19 cm, where the x- and y-axes are in the horizontal plane of the TA and the z-axis points perpendicularly away from the TA. Within this clinical tracking volume, starting at 8 cm offset with respect to the TA, single transponder position accuracy has been reported to range from 0.004 to 0.035 cm (average Euclidean distance) and single transponder precision from 0.0006 to 0.042 cm standard deviation [30]. Varian provided us with a transponder system for research which has an extended tracking volume of about 27.5 × 27.5 × 22.5 cm, starting at 5.5 cm offset. This research system also allows access to single transponder position information.

NDI Polaris Spectra

The NDI Polaris Spectra (Northern Digital Inc, Waterloo, Canada), a flexible optical tracking system (OTS) with passive reflective markers, was used as a reference for absolute accuracy assessment. This OTS has a specified root-mean-square error (RMSE) of < 0.025 cm for single optical markers, and for volumetric tools, consisting of multiple optical markers, the RMSE is < 0.017 cm [31]. This reference accuracy is considered sufficient when investigating possible submillimeter accuracy, as done in this study.

Measurement setup

The measurement setup was developed in-house, made of polyoxymethylene (POM) material and designed for single transponder accuracy assessment (manufacturing accuracy between 0.005 and 0.01 cm). The TA was fixed in a sleeve with the EM field pointing upwards, as shown in Fig. 1a.

The POM components of the setup on top of the sleeve were designed to shift the transponders throughout the entire extended tracking volume, conforming to a 3D grid of step size 2.5 cm. This step size was considered sufficiently small and facilitates comparison with the study of Franz et al. [28], who also used this step size in x- and y-directions. This resulted in 12 × 12 × 10 = 1440 transponder locations. Horizontal transponder shifting was realized by moving a black cube, in which the transponders were embedded, over a Hummelboard with 2.5 cm spaced holes (drilling accuracy < 0.001 cm) [28, 32]. The black cube, of size 10 × 10 × 4 cm, was mounted into these holes and is referred to as transponder phantom (Fig. 1b). The transponder phantom had three cylindrical holes in which rods were inserted, spaced 2.5 cm apart. Each rod contained one transponder with its readout point exactly in the center of the rod (Fig. 1c).

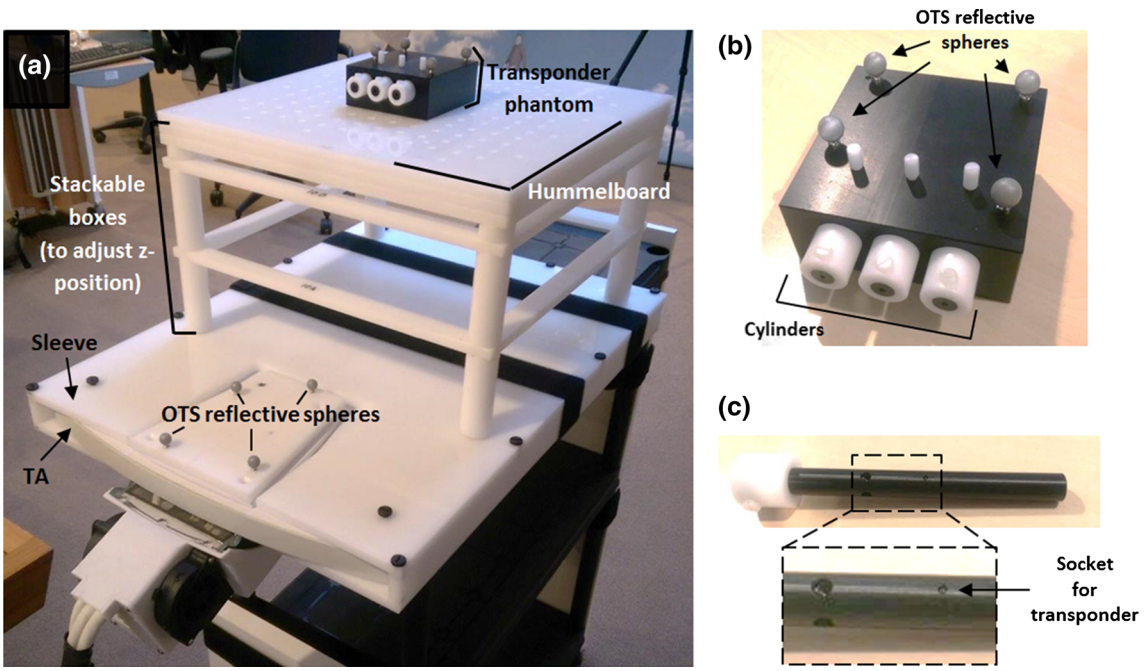

Fig. 1 Pictures of the measurement setup (**a**), the transponder phantom (**b**) and one cylinders of the transponder phantom (**c**)

Fig. 2 Setup for OR measurements. On the left a picture showing the complete setup environment and camera position. On the right a zoomed in picture of the measurement setup fastened on the OR tabletop with Velcro and showing the feet to adjust Z_{Table}

The rods are designed to rotate the transponders and fix them in a horizontal or vertical orientation. Shifting the transponders in vertical direction, i.e., in z-direction, was realized by using stackable boxes underneath the Hummelboard (Fig. 1a).

To be able to determine the transponder positions out of the OTS data, four OTS-detectable passive reflective markers were incorporated onto the transponder phantom with known configuration with respect to transponders (accuracy between 0.005 and 0.01 cm). This also allows for calibrating the transponder system (EMTS) and OTS system. However, when moving the OTS camera or the TA after the calibration, i.e., moving the OTS with respect to the EMTS global coordinate system, this calibration is not valid anymore. Therefore, another group of four passive reflective markers were mounted to the TA and the OTS transponder positions were always determined with respect to the coordinate system these spheres defined.

Data acquisition

We acquired transponder data at all 1440 single transponder locations of the 3D grid, using our custom-made software. Data of three transponders were collected simultaneously, covering 3 locations of the 3D grid. The sampling rate was 8 Hz per transponder, and 150 samples were recorded per transponder location. The OTS data were acquired and recorded similarly. All tracking information was communicated using OpenIGTLink TRANSFORM messages. For readout of the NDI hardware of the OTS and the EMTS, PlusServer from the Plus Toolkit (https://plustoolkit.github.io/) was used [33]. The software used the OpenIGTLink.dll from IGSTK (www.igstk.org) to receive and translate the OpenIGTLink messages. Within PlusServer the data for the OTS and EMTS were combined into one data stream. The OTS was connected to a laptop (dual-core 2.4 GHz Intel Core i7 5500U with 16 GB memory) using an USB 3.0 connection. The EMTS was connected to the same laptop using a local area network connection with TCP/IP communication.

Measurements

The grid measurements were first performed in a DFR, acting as a benchmark for the OR measurements. The DFR measurements were repeated for three different transponder orientations: parallel to the x-, y- and z-axes of the transponder system.

In the OR, the setup was built to simulate clinically realistic surgical procedures in the pelvic area, for example during rectal cancer surgery [17]. The TA was positioned on top of the OR tabletop with the EM field pointing upwards and the TA cables running between the leg supports (Fig. 2). Given this TA orientation, the transponders will most likely be more or less parallel to the y-axis of TA when implanted in the pelvic area. The y-axis transponder orientation is therefore selected for the OR measurements. Tracking accuracy was evaluated on two tabletop types, both developed by Maquet (Rastatt, Germany): a carbon fiber tabletop and a regular stainless steel tabletop. The carbon fiber tabletop is preferred over a regular tabletop in a surgical navigation setting with intraoperative imaging. However, also the carbon tabletop is known to interfere with the transponder system [29]. Since the amount of distortion strongly decreases with

increasing TA to OR tabletop distance [27], the grid measurement was repeated for four TA to tabletop distances, i.e., $Z_{\text{Table}} = 8.5$, 12.5, 16.5 and 20.5 cm where Z_{Table} is the distance between the top surface of the OR tabletop and the top surface of the TA (on the side of the functional EM field). All other potentially distorting components in the OR were kept at the same position over all measurements performed. Clinically realistic positions were chosen for all components in the OR, e.g., lights, monitors and leg supports.

Outcome measures

For each transponder location in the 3D grid, the absolute and relative accuracies and jitter were calculated. These outcome measures were summarized per level, i.e., per 2.5 cm step in z-direction, by calculating the RMSE over all error values measured at that level.

The absolute accuracy was defined as the vector difference between the average of the transponder position samples recorded with the EMTS and those recorded with the OTS. The relative accuracy was defined as the known physical distance subtracted by the distance measured with the EMTS in the corresponding direction. We evaluated 2.5 cm distances, obtaining $11 \times 12 \times 2 = 264$ relative accuracy values per level (covering x- and y-directions). The jitter was calculated by determining the standard deviation (SD) in each orthogonal direction and then calculating the RMS of these three SD values.

All outcome measures were calculated for the extended FoV and the clinical FoV. Per level in z-direction, transponder measurements were defined as outliers when they exceeded 3 times the interquartile range (IQR) of the error value dataset at that level [34]. Outliers were excluded from the plotted results, but the number and locations of these outliers were reported.

Calibration of EMTS and OTS

For the calibration, the DFR data obtained of both the EMTS and OTS system were selected within the range of $X_{\text{Tr}} = -6.25$ to 6.25 cm, $Y_{\text{Tr}} = -6.25$ to 6.25 cm and $Z_{\text{Tr}} = 10.5$ to 18 cm, where X_{Tr}, Y_{Tr} and Z_{Tr}, respectively, represent the x-, y- and z-transponder position values in the EMTS coordinate system. The OTS transponder position data were transformed into the optical reference coordinate system (REF) which was defined by the four reflective markers mounted to the TA. With the OTS transponder position data expressed in the REF, the positioning of the OTS camera was flexible with respect to the TA (and vice versa) after the calibration. Using a least-squares fitting point match algorithm, with the OTS and EMTS transponder position data as inputs, the transformation matrix to get from OTS to EMTS coordinates was determined. The average vector RMS error of this fit was used as the measure for the calibration accuracy.

Calibration of OR distortion using OR measurement results

To evaluate reproducibility of the distortion in the OR, the OR measurements for both OR tabletops were repeated. The absolute error vectors, including directional information, of the first OR grid measurement were subtracted from the results of the repeated OR measurement, and the residual errors were evaluated. The OR grid measurement was only repeated for Z_{Table} at which most distortion was found.

Results

The calibration of the OTS and EMTS resulted in an average vector RMSE of 0.03 cm. Due to the strong constraints of the optical object definition of the transponder phantom, an optimal view of the OTS camera on the transponder phantom was required. Therefore, the camera had to be repositioned a few times during the measurements.

DFR measurements

In the clinical FoV, the absolute and relative accuracies and the jitter showed little to no difference over the different transponder orientations, for transponder to TA distances (Z_{Tr}) of 10.5 cm and higher (Fig. 3).

In both the clinical and extended FoV, the absolute and relative accuracies stayed well within 0.1 cm RMS. The jitter in the clinical FoV also stayed well below 0.1 cm for all orientations, up to $Z_{\text{Tr}} = 25.5$ cm, and at $Z_{\text{Tr}} = 28$ cm the jitter was around 0.2 cm. The jitter in the extended FoV was higher with respect to the clinical FoV for the x-axis and y-axis transponder orientation from $Z_{\text{Tr}} = 18$ cm to $Z_{\text{Tr}} = 28$ cm. In that range the jitter increased from 0.1 cm to 0.4 cm, respectively, for the y-axis orientation and similarly for the x-axis orientation except for the peak of 0.9 cm at $Z_{\text{Tr}} = 28$ cm.

In the clinical FoV, outliers were only detected at $Z_{\text{Tr}} = 8$ cm for the x-axis and z-axis transponder orientations (Table 1). In the extended FoV, the absolute and relative number of outliers was higher at this level. Also at one level lower (at $Z_{\text{Tr}} = 5.5$ cm) and at $Z_{\text{Tr}} \geq 23$ cm outliers were detected. Most of the outliers at the higher levels were found for the x-axis and y-axis transponder orientation at the edge of the FoV at $y = -13.75$ cm. A visualization of the absolute errors (including outliers) throughout the extended FoV is shown in Fig. 4.

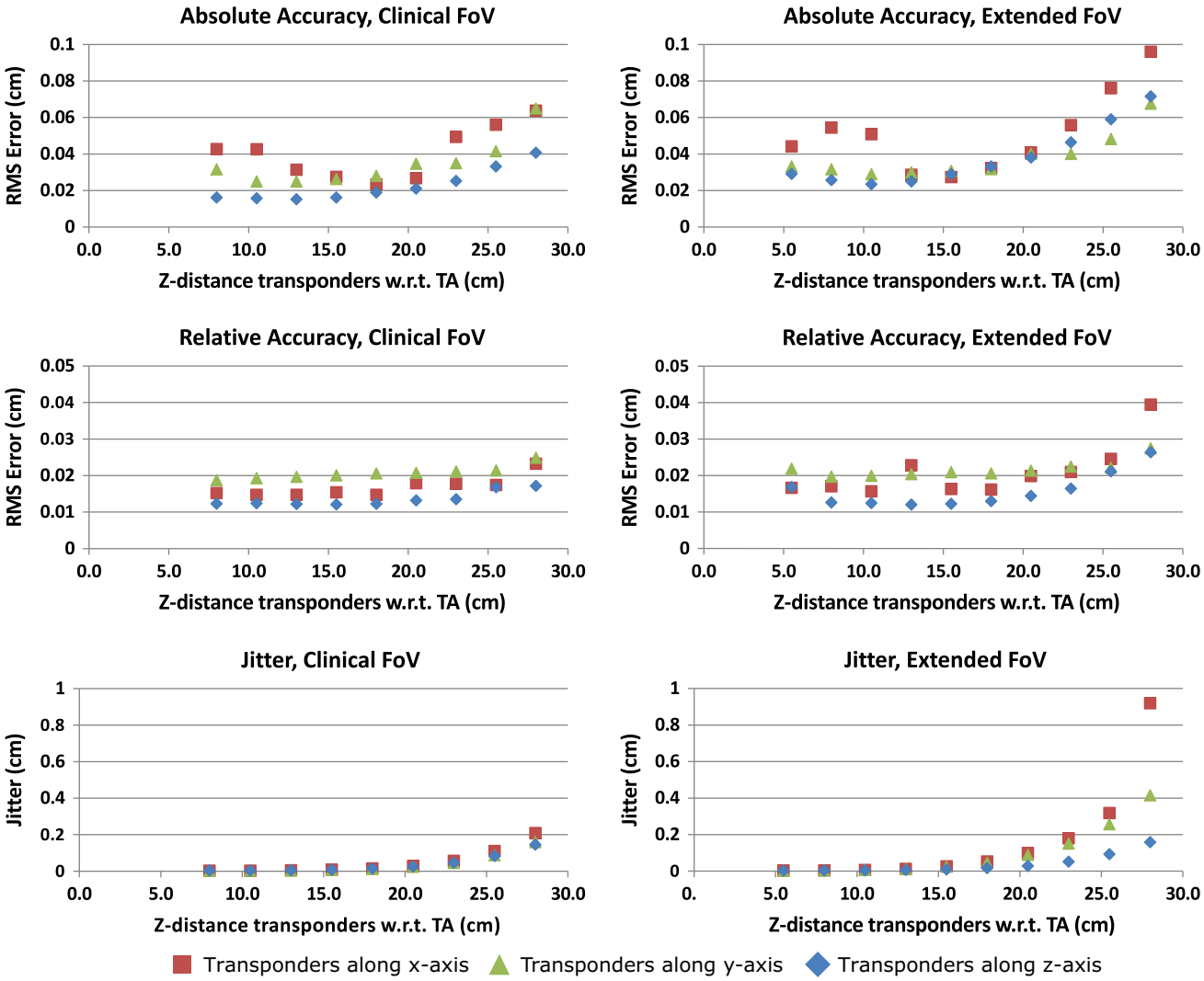

Fig. 3 The DFR results of, from top to down, the absolute accuracy, the relative accuracy and the jitter, plotted against the z-distance of the transponders with respect to the EM tracking array. On the left the plots for the clinical FoV and on the right the plots for the extended FoV. The three different colors represent the three transponder orientations

OR measurements

Carbon tabletop results

In the OR, the relative accuracy and jitter results for all Z_{Table} distances, except $Z_{\text{Table}} = 8.5$ cm, on the carbon tabletop were very similar to the DFR results, as shown in Fig. 5.

The distortion effect of the carbon fiber tabletop was evident in the absolute accuracy results, with the biggest errors above 1 cm, whereas the effect was negligible for the jitter and relative accuracy for Z_{Table} larger than 8.5 cm. The absolute accuracy strongly decreased with increasing Z_{Table}, for both the clinical and the extended FoV. For $Z_{\text{Tr}} \geq 20.5$ cm the biggest errors were found for transponder locations close to the edges of the FoV in negative and positive y-direction.

No outliers were detected in the clinical FoV except for 4 outliers at $Z_{\text{Tr}} = 8$ cm at $Z_{\text{Table}} = 12$ cm. The amount and location of the outliers found in the extended FoV were similar as found in DFR data.

Regular table results

Similar to the OR measurement results with the carbon fiber tabletop, the relative accuracy and jitter results of the measurements with the regular tabletop were very similar to the DFR results (not shown). This applied to the clinical as well as the extended FoV. The absolute accuracy results again showed that increasing Z_{Table} clearly decreases the absolute errors (Fig. 6). The distortion due to the regular tabletop is clearly less than the carbon fiber tabletop distortion, espe-

Table 1 Overview of the outliers in DFR data, separated for the clinical and extended FoV

z-distance transponders w.r.t. TA (cm)	# Outliers in clinical FoV (% out of 36 positions)			# Outliers in extended FoV (% out of 144 positions)		
	x-axis orientation	*y*-axis orientation	*z*-axis orientation	*x*-axis orientation	*y*-axis orientation	*z*-axis orientation
5.5				6 (4%)	6 (4%)	7 (5%)
8	3 (8%)		6 (17%)	19 (13%)	6 (4%)	22 (15%)
10.5						1 (<1%)
13				1 (<1%)		
15.5						
18						
20.5						
23				3 (2%)	8 (6%)	
25.5				5 (3%)	12 (8%)	
28				19 (13%)	21 (15%)	2 (1%)

The rows represent the different transponder to TA levels and the columns the three different beacon orientations. Empty cells represent zero outliers

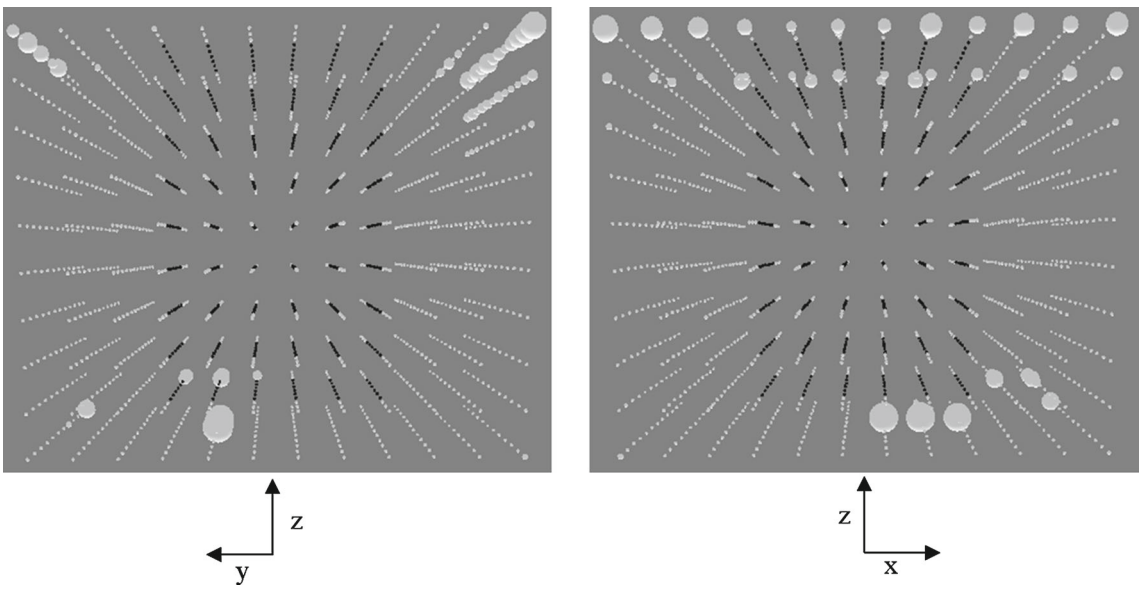

Fig. 4 3D visualization of the absolute errors, as found in the DFR, throughout the extended FoV for *y*-axis transponder orientation. Each sphere represents one measurement location in the 3D measurement grid and the sphere radius is proportional to the absolute error at that specific location, the bigger the radius the bigger the absolute error. For visibility, the smallest dot diameter is 0.1 cm, representing errors equal to or smaller than 0.1 cm, and the maximum dot diameter is 1 cm. The black spheres indicate these measurements were within the clinical FoV. On the left the view in positive x-direction of the EMTS and on the right the view in positive *y*-direction

cially for larger transponder to TA distances. Outliers were detected in similar amounts and at similar regions within the FoV compared to the carbon tabletop measurements.

Calibration of OR distortion

The grid measurement was repeated on the carbon fiber tabletop at $Z_{\text{Table}} = 12.5$ cm and on the regular tabletop at $Z_{\text{Table}} = 8.5$ cm. The higher Z_{Table} for the carbon tabletop was required because we found, during the DFR measurements, that the

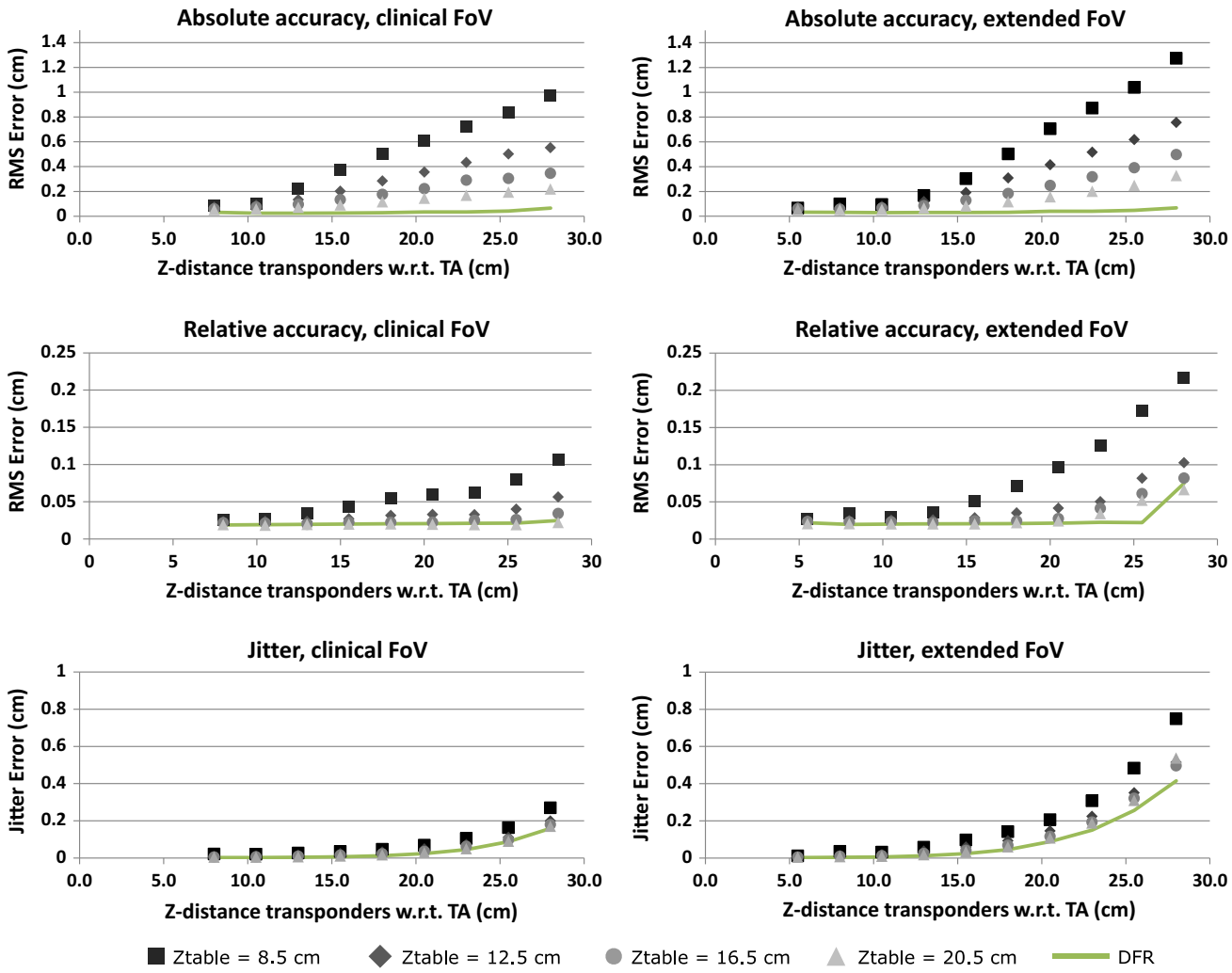

Fig. 5 Results OR measurements with Carbon fiber tabletop. From top to down: the absolute accuracy, the relative accuracy and the jitter in cm, plotted against the z-distance of the transponders with respect to the EM tracking array. On the left the plots for the clinical FoV and on the right the plots for the extended FoV

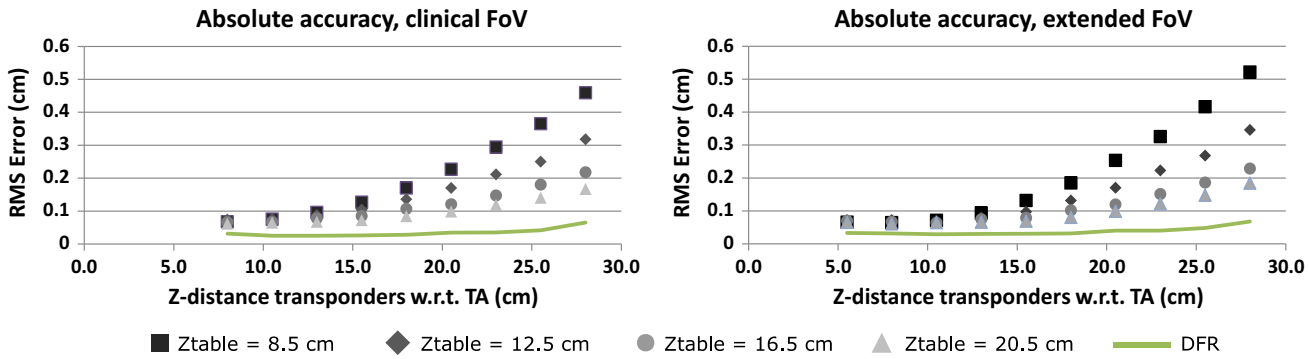

Fig. 6 Results OR measurements with regular tabletop. On the left the absolute accuracy results for the clinical FoV and on the right a similar plot for the extended FoV, errors plotted against the z-distance of the transponders with respect to the EM tracking array

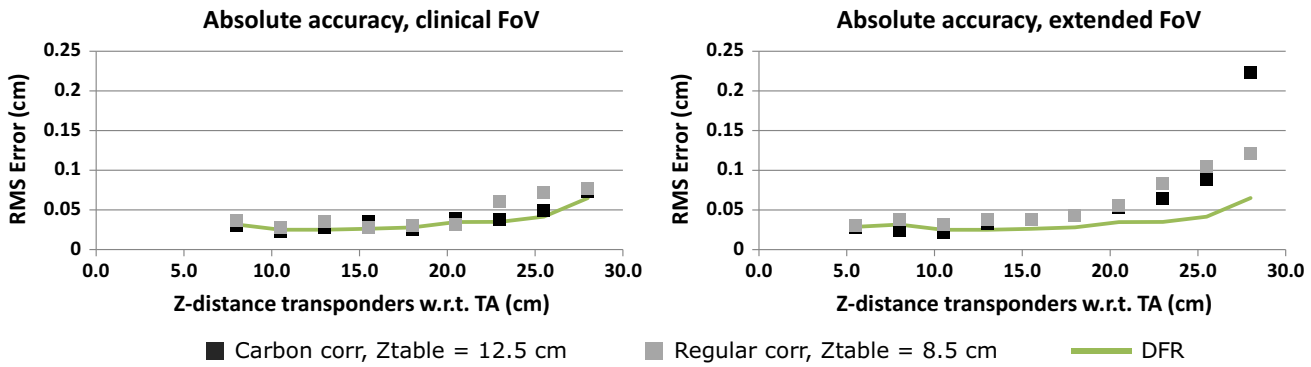

Fig. 7 Effect of correcting for absolute errors caused by a carbon and regular OR tabletop at $Z_{\text{Table}} = 12.5$ cm and 8.5 cm, respectively

temperature of the carbon tabletop would get too high at shorter Z_{Table} distances. Eddy currents in the carbon material, induced by the EM field, are the cause of this temperature rise. The results of the repeated OR grid measurement, with the absolute errors of the first OR grid measurement subtracted, are plotted in Fig. 7.

For the clinical FoV, correcting for the OR tabletop distortion resulted in absolute errors almost identical to those found in the DFR measurements. Up to $Z_{\text{Tr}} = 20.5$ cm, this also applied to the extended FoV and the RMS error stayed below 0.1 cm up to $Z_{\text{Tr}} = 25.5$ cm.

Discussion

In the DFR, the relative and absolute accuracies within the extended FoV ($27.5 \times 27.5 \times 22.5$ cm) were very similar to what we found for the clinical FoV ($14 \times 14 \times 19$ cm), although outliers were detected toward the edges of the tracking volume. Excluding these outliers, a relative and absolute accuracy of 0.1 cm RMSE could still be achieved in these regions, which is similar to the accuracy of wired EM tracking alternatives [35, 36]. There was little to no difference in jitter between the clinical and extended FoV for the z-axis orientation, whereas the x-axis and y-axis orientation showed increased jitter in the extended FoV. The OR tabletops mainly influenced the absolute accuracy, but this was reproducible and could therefore be calibrated.

A standardized accuracy assessment protocol was used to assess single transponder accuracy, comparable to Franz et al. [28]. DFR results (Fig. 3) for the clinical FoV in the current study are similar to their results: relative accuracy and jitter increased with increasing transponder to TA distance, but stayed below 0.1 cm RMS. Furthermore, tracking problems were encountered for x-axis transponder orientations at the level closest to the edge of the clinical FoV, i.e., $Z_{\text{Tr}} = 8$ cm, and transponder orientation had very little effect on the relative accuracy and jitter. In contrast to the study of Franz et al., we also assessed accuracy for an extended FoV, included absolute accuracy, measured at more levels (along the z-axis) and repeated the assessment in an OR environment.

The extended FoV results were similar to the clinical FoV (Fig. 3), although transponder outliers can be expected for $Z_{\text{Tr}} < 10.5$ cm and $Z_{\text{Tr}} > 20.5$ cm. However, since the transponder system calculates the isocenter of three transponders, these outliers may be filtered out. Also, the risk and therefore impact of these single transponder outliers can be limited by avoiding the edges of the tracking volume at these levels, especially in the outer y-directions. Figure 4 visualizes these inaccurate regions. During actual surgery, outliers could be detected by putting constraints on the inter-individual transponder distances or on the RMSE for registering the transponders to their implantation position. The jitter in the extended FoV for the z-axis orientation was similar to the jitter in the clinical FoV, whereas for the other orientations the jitter was clearly higher, especially for the x-axis orientation at $Z_{\text{Tr}} = 28$ cm. To mitigate this increased jitter, a Savitzky–Golay filter can be used. The absolute accuracy in the extended FoV was within submillimeter range inside the DFR, indicating the transponder system can be used with high accuracy in combination with a second system to track surgical tools.

In the OR measurements, decreasing the TA to OR tabletop distances highly reduced the absolute accuracy, resulting in errors up to several millimeters and even above 1 cm for a carbon tabletop at the largest transponder to TA distances assessed (Figs. 5, 6). The distortion was reproducible and could be calibrated, achieving an accuracy of RMSE of < 0.1 cm within the extended FoV up to 25 cm above the TA (Fig. 7). The distortion of the OR tabletops on the relative accuracy was limited and stayed below 0.1 cm RMSE without calibrating the distortion. This means that in OR settings where a second tracking system is not required to track surgical tools and the distance between transponder positions will be relatively small, the transponder system can be used with high accuracy without having to calibrate for distortion. In this study, all three available transponders were

assumed to be implanted inside the tumor area to derive position and orientation data of the tumor. However, when only positional information of the tumor is sufficient, navigation using only three transponders seems feasible, for example by using two of the transponders to track the surgical tool. It is technically possible to track more than three transponders with the transponder system, however, the system sampling rate is 25 Hz, forcing a reduction in the sampling rate per transponder with more transponders. A lower sampling rate per transponder will lower the refreshment rate of a surgical navigation interface, limiting the intuitive and efficient interaction of the surgeon with the interface. Also, when using transponders to track a surgical tool, the influence on tracking accuracy when transponders are in close proximity to that tool, should be investigated. However, from our experience, e.g., during the study of Janssen et al. [26], this influence is negligible.

Assuming a setting where the transponder system is used to track tumor position as well as tumor orientation, the Polaris system may be used as a second tracking system to track surgical tools, since the two tracking systems could be aligned with 0.03 cm RMSE. Furthermore, the optical markers accompanying this OTS can be used in a sterile environment. In the calibration of the OTS with the EMTS, the data of optical markers mounted onto the TA were integrated (Fig. 1a), so the camera and the TA could move relatively to each other without having to recalibrate. In a clinical OR setting, the optical markers on the TA would be underneath surgical draping, so an alternative location of these markers, with a rigid connection to the TA, should be selected or created. When a clinical navigation setup using the OTS and EMTS can be designed, the next step is to find a method to correct for the OR tabletop distortion. This can be done by preoperatively deriving a calibration set of this distortion and use it intraoperatively, as long as the relative TA to tabletop position is the same in both situations. In this study, data used to calibrate the tabletop influence on accuracy were acquired at the minimal TA to tabletop distances, respectively, 8.5 and 12.5 cm for the regular and the carbon tabletop. Smaller distances were not possible because of the construction of the regular tabletop and the temperature rise of the carbon tabletop at lower distances. When adding the minimally required Z_{Tr} of 5.5 cm (start of FoV), the patient to tabletop distance has to be 14 and 18 cm for the regular and carbon tabletop, respectively. With a custom-made thicker mattress, having the TA inserted into it [37], the increase in patient to tabletop distance can be reduced to 6 and 10 cm, given that the standard patient to tabletop distance is 8 cm. This is acceptable when the custom-made mattress has sufficient firmness.

In the OR measurements single transponder accuracy was assessed for the *y*-axis orientation only, because it is the most likely transponder orientation for pelvic applications. The absolute tracking accuracy and its reproducibility are expected to be similar for other orientations. Similarly, it is expected that the relative accuracy and jitter in the DFR for other transponder orientations than the three orthogonal orientations measured will not show significantly deviating results. Further research is needed to verify these assumptions. Another limitation of this study is that mainly the influence of the OR tabletop was assessed, while there are more sources of distortion in the OR. Calibration for other sources of distortion can be challenging, especially for dynamic objects such as surgical tools. Franz et al. [28] found that the accuracy can decrease with a few millimeters RMS even when a metal object is about 5 cm away from the transponders. However, in their setup the metal objects were between the TA and the transponders, whereas this is less likely to occur in the current proposed clinical setup because the patient lies on top of the TA.

Our findings show that transponder accuracy within the extended FoV is comparable to the accuracy of other wired EM tracking techniques, even in proximity of the tested OR tabletops after calibrating for their distortion, and that it can be used together with an OTS for tool tracking. A clinical workflow, for using transponders to track tumor motion, already exists for RT and is therefore relatively easy to implement for surgery. Our breast phantom study on transponder-based surgery also showed the potential of improving intraoperative awareness of preoperatively defined tumor borders and surgeons were enthusiastic about the possibilities [26]. Transponder-based tracking techniques are promising for surgery on tumors in non-rigid target areas. In future research, the reproducibility of the OR tabletop distortion for more transponder orientations and the effect of other metal objects on the accuracy will be investigated. Furthermore, a feasible clinical setup using the EMTS with the OTS within the OR will be designed.

Conclusions

This study presents a navigation setup for surgical procedures in the pelvic area, in which wireless transponder tracking can be used for tumor motion tracking. Tracking accuracy is dependent on the distance between the transponders and the tracking array and is also dependent on the distance between the OR table and the tracking array. The influence of the OR tabletop on the accuracy is reproducible and can therefore be compensated for by a calibration procedure. Prerequisite for this is a sensor array to OR tabletop distance of at least 14 cm for a regular tabletop and 18 cm for a carbon tabletop. After calibration, the extended field of view can be used with a tracking accuracy of 0.1 cm RMSE over the full horizontal range of 27.5×27.5 cm for transponder to sensor array distances up to 25 cm. A flexible optical tracking system was successfully integrated into the navigation setup, allow-

ing for tracking surgical tools while transponders track the tumor during surgery. These are encouraging results to further develop wireless transponder-based tumor tracking for surgical navigation.

Acknowledgments We would like to thank Ton Vlasveld for his help in fabricating the measurement setup and Professor Jan-Jakob Sonke for his insightful input. We would like to thank Koningin Wilhelmina Fonds - Alpe d'HuZes (NKI 2014-6596) for their funding.

Funding This study was funded by KWF-Alpe d'HuZes (NKI 2014-6596)

Compliance with ethical standards

Conflict of interest The Netherlands Cancer Institute that facilitated this research has a research agreement with Varian Medical Systems. Varian was not involved in the design or execution of the study.

Human and animal rights This article does not contain any studies with human participants or animals performed by any of the authors.

References

1. Senft C, Ulrich CT, Seifert V, Gasser T (2010) Intraoperative magnetic resonance imaging in the surgical treatment of cerebral metastases. J Surg Oncol 101:436–441
2. Ochs BG, Schreiner AJ, de Zwart PM, Stockle U, Gonser CE (2016) Computer-assisted navigation is beneficial both in primary and revision surgery with modular rotating-hinge knee arthroplasty. Knee Surg Sports Traumatol Arthrosc 24:64–73
3. Lango T, Tangen GA, Marvik R, Ystgaard B, Yavuz Y, Kaspersen JH, Solberg OV, Hernes TA (2008) Navigation in laparoscopy—prototype research platform for improved image-guided surgery. Minim Invasive Ther Allied Technol 17:17–33
4. Aschendorff A, Maier W, Jaekel K, Wesarg T, Arndt S, Laszig R, Voss P, Metzger M, Schulze D (2009) Radiologically assisted navigation in cochlear implantation for X-linked deafness malformation. Cochlear Implant Int 10(Suppl 1):14–18
5. Galloway RL, Herrell SD, Miga MI (2012) Image-guided abdominal surgery and therapy delivery. J Healthc Eng 3:203–228
6. Simpson AL, Kingham TP (2016) Current evidence in image-guided liver surgery. J Gastrointest Surg 20:1265–1269
7. Kingham TP, Scherer MA, Neese BW, Clements LW, Stefansic JD, Jarnagin WR (2012) Image-guided liver surgery: intraoperative projection of computed tomography images utilizing tracked ultrasound. HPB 14:594–603
8. Peterhans M, vom Berg A, Dagon B, Inderbitzin D, Baur C, Candinas D, Weber S (2011) A navigation system for open liver surgery: design, workflow and first clinical applications. Int J Med Robot 7:7–16
9. Su LM, Vagvolgyi BP, Agarwal R, Reiley CE, Taylor RH, Hager GD (2009) Augmented reality during robot-assisted laparoscopic partial nephrectomy: toward real-time 3D-CT to stereoscopic video registration. Urology 73:896–900
10. Sugimoto M, Yasuda H, Koda K, Suzuki M, Yamazaki M, Tezuka T, Kosugi C, Higuchi R, Watayo Y, Yagawa Y, Uemura S, Tsuchiya H, Azuma T (2010) Image overlay navigation by markerless surface registration in gastrointestinal, hepatobiliary and pancreatic surgery. J Hepatobiliary Pancreat Sci 17:629–636
11. Soler L, Nicolau S, Pessaux P, Mutter D, Marescaux J (2014) Real-time 3D image reconstruction guidance in liver resection surgery. Hepatobiliary Surg Nutr 3:73–81
12. Suwelack S, Rohl S, Bodenstedt S, Reichard D, Dillmann R, dos Santos T, Maier-Hein L, Wagner M, Wunscher J, Kenngott H, Muller BP, Speidel S (2014) Physics-based shape matching for intraoperative image guidance. Med Phys 41:111901
13. Collins JA, Weis JA, Heiselman JS, Clements LW, Simpson AL, Jarnagin WR, Miga MI (2017) Improving registration robustness for image-guided liver surgery in a novel human-to-phantom data framework. IEEE Trans Med Imaging 36:1502–1510
14. Rucker DC, Wu Y, Clements LW, Ondrake JE, Pheiffer TS, Simpson AL, Jarnagin WR, Miga MI (2014) A mechanics-based nonrigid registration method for liver surgery using sparse intraoperative data. IEEE Trans Med Imaging 33:147–158
15. Wild E, Teber D, Schmid D, Simpfendorfer T, Muller M, Baranski AC, Kenngott H, Kopka K, Maier-Hein L (2016) Robust augmented reality guidance with fluorescent markers in laparoscopic surgery. Int J Comput Assist Radiol Surg 11:899–907
16. Franz AM, Haidegger T, Birkfellner W, Cleary K, Peters TM, Maier-Hein L (2014) Electromagnetic tracking in medicine–a review of technology, validation, and applications. IEEE Trans Med Imaging 33:1702–1725
17. Wagner M, Gondan M, Zollner C, Wunscher JJ, Nickel F, Albala L, Groch A, Suwelack S, Speidel S, Maier-Hein L, Muller-Stich BP, Kenngott HG (2016) Electromagnetic organ tracking allows for real-time compensation of tissue shift in image-guided laparoscopic rectal surgery: results of a phantom study. Surg Endosc 30:495–503
18. Ungi T, Gauvin G, Lasso A, Yeo CT, Pezeshki P, Vaughan T, Carter K, Rudan J, Engel CJ, Fichtinger G (2016) Navigated breast tumor excision using electromagnetically tracked ultrasound and surgical instruments. IEEE Trans Biomed Eng 63:600–606
19. Willoughby TR, Kupelian PA, Pouliot J, Shinohara K, Aubin M, Roach M 3rd, Skrumeda LL, Balter JM, Litzenberg DW, Hadley SW, Wei JT, Sandler HM (2006) Target localization and real-time tracking using the Calypso 4D localization system in patients with localized prostate cancer. Int J Radiat Oncol Biol Phys 65:528–534
20. Zhu M, Bharat S, Michalski JM, Gay HA, Hou WH, Parikh PJ (2013) Adaptive radiation therapy for postprostatectomy patients using real-time electromagnetic target motion tracking during external beam radiation therapy. Int J Radiat Oncol Biol Phys 85:1038–1044
21. Zhang P, Hunt M, Happersett L, Yang J, Zelefsky M, Mageras G (2013) Robust plan optimization for electromagnetic transponder guided hypo-fractionated prostate treatment using volumetric modulated arc therapy. Phys Med Biol 58:7803–7813
22. Sawant A, Smith RL, Venkat RB, Santanam L, Cho B, Poulsen P, Cattell H, Newell LJ, Parikh P, Keall PJ (2009) Toward submillimeter accuracy in the management of intrafraction motion: the integration of real-time internal position monitoring and multileaf collimator target tracking. Int J Radiat Oncol Biol Phys 74:575–582
23. Kupelian P, Willoughby T, Mahadevan A, Djemil T, Weinstein G, Jani S, Enke C, Solberg T, Flores N, Liu D, Beyer D, Levine L (2007) Multi-institutional clinical experience with the Calypso system in localization and continuous, real-time monitoring of the prostate gland during external radiotherapy. Int J Radiat Oncol Biol Phys 67:1088–1098
24. Sonnenday CJ, Kaufman HS (2003) Use of an implantable marker for rapid intraoperative localization of nonpalpable tumors: a pilot study in a swine colorectal model. Surg Endosc 17:1927–1931
25. Nakamoto M, Ukimura O, Gill IS, Mahadevan A, Miki T, Hashizume M, Sato Y (2008) Realtime organ tracking for endoscopic augmented reality visualization using miniature wireless magnetic tracker. MIAR 5128:359–366

26. Janssen N, Eppenga R, Peeters MV, van Duijnhoven F, Oldenburg H, van der Hage J, Rutgers E, Sonke JJ, Kuhlmann K, Ruers T, Nijkamp J (2018) Real-time wireless tumor tracking during breast conserving surgery. Int J Comput Assist Radiol Surg 13:531–539
27. Nafis C, Jensen V, Von Jako R (2008) Method for evaluating compatibility of commercial electromagnetic (EM) microsensor tracking systems with surgical and imaging tables. Med Imaging 6918(691820):15
28. Franz AM, Schmitt D, Seitel A, Chatrasingh M, Echner G, Oelfke U, Nill S, Birkfellner W, Maier-Hein L (2014) Standardized accuracy assessment of the calypso wireless transponder tracking system. Phys Med Biol 59:6797–6810
29. Wen J (2010) Electromagnetic tracking for medical imaging. All Theses and Dissertations (ETDs) Paper 469, Washington University, Saint Louis
30. Balter JM, Wright JN, Newell LJ, Friemel B, Dimmer S, Cheng Y, Wong J, Vertatschitsch E, Mate TP (2005) Accuracy of a wireless localization system for radiotherapy. Int J Radiat Oncol Biol Phys 61:933–937
31. Elfring R, de la Fuente M, Radermacher K (2010) Assessment of optical localizer accuracy for computer aided surgery systems. Comput Aided Surg 15:1–12
32. Hummel J, Figl M, Kollmann C, Bergmann H, Birkfellner W (2002) Evaluation of a miniature electromagnetic position tracker. Med Phys 29:2205–2212
33. Lasso A, Heffter T, Rankin A, Pinter C, Ungi T, Fichtinger G (2014) PLUS: open-source toolkit for ultrasound-guided intervention systems. IEEE Trans Biomed Eng 61:2527–2537
34. Tukey JW (1977) Exploratory data analysis. Pearson, Don Mills
35. Nijkamp J, Schermers B, Schmitz S, de Jonge S, Kuhlmann K, van der Heijden F, Sonke JJ, Ruers T (2016) Comparing position and orientation accuracy of different electromagnetic sensors for tracking during interventions. Int J Comput Assist Radiol Surg 11:1487–1498
36. Nafis C, Jensen V, Beauregard L, Anderson P (2006) Method for estimating dynamic EM tracking accuracy of surgical navigation tools. Proc SPIE Int Soc Opt Eng 6141:152–167
37. Nijkamp J, Kuhlmann K, Sonke J-J, Ruers T (2016) Image-guided navigation surgery for pelvic malignancies using electromagnetic tracking and intra-operative imaging. Int J Comput Assist Radiol Surg 11:2